Available online at www.sciencedirect.com

ScienceDirect

Nuclear Physics B 940 (2019) 292–311

NUCLEAR PHYSICS B

www.elsevier.com/locate/nuclphysb

Neutrino mass in a gauged $L_\mu - L_\tau$ model

Chuan-Hung Chen [a], Takaaki Nomura [b,*]

[a] *Department of Physics, National Cheng-Kung University, Tainan 70101, Taiwan*
[b] *School of Physics, KIAS, Seoul 02455, Republic of Korea*

Received 15 June 2018; received in revised form 13 December 2018; accepted 26 January 2019
Available online 31 January 2019
Editor: Hong-Jian He

Abstract

We study the origin of neutrino mass through lepton-number violation and spontaneous $U(1)_{L_\mu - L_\tau}$ symmetry breaking. To accomplish the purpose, we include one Higgs triplet, two singlet scalars, and two vector-like doublet leptons in the $U(1)_{L_\mu - L_\tau}$ gauge extension of the standard model. To completely determine the free parameters, we employ the Frampton–Glashow–Marfatia (FGM) two-zero texture neutrino mass matrix as a theoretical input. It is found that when some particular Yukawa couplings vanish, an FGM pattern can be achieved in the model. Besides the explanation of neutrino data, we find that the absolute value of neutrino mass m_j can be obtained in the model, and their sum can satisfy the upper bound of the cosmological measurement with $\sum_j |m_j| < 0.12$ eV. The effective Majorana neutrino mass for neutrinoless double-beta decay is below the current upper limit and is obtained as $\langle m_{\beta\beta} \rangle = (0.34,\ 2.3) \times 10^{-2}$ eV. In addition, the doubly charged Higgs $H^{\pm\pm}$ decaying to $\mu^\pm \tau^\pm$ final states can be induced from a dimension-6 operator and is not suppressed, and its branching ratio is compatible with the $H^{\pm\pm} \to W^\pm W^\pm$ decay when the vacuum expectation value of Higgs triplet is $O(0.01)$ GeV.

1. Introduction

In spite of the mass hierarchy among the quarks and charged leptons, the particle masses, with the exception of the neutrinos, in the standard model (SM) can be attributed to the Brout–Englert–

* Corresponding author.
E-mail addresses: physchen@mail.ncku.edu.tw (C.-H. Chen), nomura@kias.re.kr (T. Nomura).

https://doi.org/10.1016/j.nuclphysb.2019.01.016

Higgs (BEH) mechanism [1,2], where the predicted Higgs boson is observed using ATLAS [3] and CMS [4] at a mass of 125 GeV. Based on the neutrino oscillation experiments, it is found that the neutrinos are also massive particles; however, the definite origin of their masses so far is unknown.

Moreover, although nonzero neutrino masses have been determined by the experiments, we still cannot tell their mass order, i.e., $|m_1| < |m_2| < |m_3|$ or $|m_3| < |m_1| < |m_2|$ is possible, where the former and latter are the mass spectrum with normal ordering (NO) and inverted ordering (IO), respectively. Hence, the current neutrino data can be shown in terms of the different mass ordering as [5]:

$$\begin{aligned}
\Delta m^2_{21} &= (7.53 \pm 0.18) \times 10^{-5}\ \text{eV}^2\,,\ \sin^2\theta_{12} = 0.304 \pm 0.014\,,\\
\Delta m^2_{32} &= (2.44 \pm 0.06,\ 2.51 \pm 0.06) \times 10^{-3}\ \text{eV}^2\ (\text{NO, IO})\,,\\
\sin^2\theta_{23} &= (0.51 \pm 0.05,\ 0.50 \pm 0.05)\ (\text{NO, IO})\,,\\
\sin^2\theta_{13} &= (2.19 \pm 0.12) \times 10^{-2}\,,
\end{aligned} \tag{1}$$

where $m^2_{21} \equiv m^2_2 - m^2_1$, m^2_{23} denotes $m^2_3 - m^2_2$ for NO or $m^2_2 - m^2_3$ for IO, and θ_{ij} are the mixing angles of the Pontecorvo–Maki–Nakagawa–Sakata (PMNS) matrix [6,7]. From the results, it is clearly seen that the PMNS matrix pattern is different from the Cabibbo–Kobayashi–Maskawa (CKM) matrix [8,9], which dictates the quark-flavor mixing. In this work, we plan to study a model, where based on a flavor symmetry, the neutrino masses are dynamically generated without introducing singlet right-handed neutrinos [10], and all neutrino data can be explained. Although it is inevitable to fine-tune the Yukawa couplings to fit the neutrino masses, the model can provide interesting phenomenological implications in flavor and collider physics.

Inspired by the experimental indication of maximal θ_{23}, large θ_{12}, and small θ_{13}, various Abelian flavor-symmetry based models have been proposed to understand the neutrino properties [11–21]. Among these flavor symmetries, we investigate the neutrino problems in an $U(1)_{L_\mu - L_\tau}$ gauge symmetry. We focus on such gauge symmetry based on some phenomenological considerations: (i) gauge anomaly-free conditions are automatically satisfied [22,23]; (ii) excess of muon anomalous magnetic dipole moment (muon $g-2$) can be resolved [24–26]; (iii) excesses in semileptonic B-meson decays can be explained [27–31]; (iv) potential signals for the processes $e^+e^- \to \gamma Z'$ [32,33] and $\tau \to \mu Z' Z'$ [34] can be observed at Belle II. Other interesting studies can be found in [35–43].

In order to dynamically generate the neutrino masses, we require that each Majorana matrix entry is related to the lepton-number violating effect and the breaking of spontaneous $U(1)_{L_\mu - L_\tau}$ symmetry. To achieve the lepton-number violation, like type-II seesaw model [44,45], we introduce a Higgs triplet, which carries a hypercharge $Y = 1$ and has no $U(1)_{L_\mu - L_\tau}$ charge. We find that due to the protection of $U(1)_{L_\mu - L_\tau}$ gauge symmetry, we cannot obtain a realistic Majorana neutrino mass matrix without further introducing the breaking of $U(1)_{L_\mu - L_\tau}$. Therefore, to break the gauge symmetry, we employ two singlet scalars, which carry different $U(1)_{L_\mu - L_\tau}$ charges. Because the lepton chirality cannot be matched, the SM leptons cannot couple to the singlet scalars; therefore, we must introduce proper exotic heavy leptons as the media. To avoid gauge anomalies, we employ two vector-like doublet leptons as the candidates. Based on the $U(1)_{L_\mu - L_\tau}$ gauge symmetry, the number of singlet scalars and vector-like leptons (VLLs) in this approach is the minimal requirement by which to obtain a proper Majorana neutrino mass matrix.

Since the number of free parameters in the Majorana neutrino mass matrix is more than that of the neutrino data, not all free parameters can be determined. In order to completely determine the

Table 1
$U(1)_{L_\mu - L_\tau}$ charges of involving leptons, S, and S'.

	e	μ	τ	L_4	L_5	Δ	S'	S
$U(1)$	0	1	−1	−1	1	0	1	2

free parameters, we employ the Frampton–Glashow–Marfatia (FGM) matrix pattern [55], which has two independent zeros, as a theoretical input.

It is demonstrated later that not all Yukawa couplings appearing in the neutrino mass matrix are small. Therefore, in addition to the neutrino issue, the model can also provide interesting phenomena related to flavor and collider physics. For instance, the lepton-flavor violating $h \to \mu\tau$ decay can be as large as the current measurements [56,57]; excess of muon $g-2$ can be resolved by the mediation of the Z' gauge boson, and the doubly charged Higgs decaying to $\mu\tau$ and WW can be compatible each other without requiring the VEV of the Higgs triplet to be the eV.

This paper is organized as follows. In Sec. 2, we introduce the model under the $SU(2)_L \times U(1)_Y \times U(1)_{L_\mu - L_\tau}$ local gauge symmetry. In Sec. 3, we generate the Majorana neutrino mass matrix without right-handed neutrinos in the model and discuss the relation to the FGM matrix pattern. The numerical analysis on neutrino physics and implications of the model on other phenomena are shown in Sec. 4. A summary is given in Sec. 4.

2. Model

In this section, we introduce the model under the $SU(2)_L \times U(1)_Y \times U(1)_{L_\mu - L_\tau}$ local gauge symmetry. In order to dynamically generate the neutrino mass in the $U(1)_{L_\mu - L_\tau}$ extension of the SM, in addition to the SM particles, we include one Higgs triplet (Δ), two vector-like doublet leptons (L_4, L_5), and two singlet scalars (S, S'). Their $U(1)_{L_\mu - L_\tau}$ charges are given in Table 1, where the SM particles not shown in the table carry no such $U(1)$ charges. Accordingly, the Yukawa couplings to the Higgs triplet are written as:

$$\begin{aligned} -\mathcal{L}_Y^\Delta = &\frac{1}{2} Y_{ee} L_e^T C i\tau_2 \Delta L_e + Y_{\mu\tau} L_\mu^T C i\tau_2 \Delta L_\tau + Y_{\mu 4} L_\mu^T C i\tau_2 \Delta L_{4L} \\ &+ Y_{\tau 5} L_\tau^T C i\tau_2 \Delta L_{5L} + Y_{45} L_{4L}^T C i\tau_2 \Delta L_{5L} + Y'_{45} L_{4R}^T C i\tau_2 \Delta L_{5R} + H.c. \end{aligned} \tag{2}$$

From the above equation, if the Higgs triplet Δ carries two lepton-number units, the Yukawa interactions are lepton-number conserved. However, when the Higgs triplet obtains a VEV, i.e. $\langle \Delta \rangle = v_\Delta / \sqrt{2}$, the lepton-number violating Majorana neutrino mass matrix for three light neutrinos is induced and expressed as:

$$M^\nu = \begin{pmatrix} \frac{Y_{ee} v_\Delta}{\sqrt{2}} & 0 & 0 \\ 0 & 0 & \frac{Y_{\mu\tau} v_\Delta}{\sqrt{2}} \\ 0 & \frac{Y_{\mu\tau} v_\Delta}{\sqrt{2}} & 0 \end{pmatrix}, \tag{3}$$

where the pattern of mass matrix leads to $m_2 = m_3$, $\theta_{13} = \theta_{12} = 0$, and $\theta_{23} = \pi/4$ [11,19,20]. Obviously, the results cannot explain the current neutrino data [5]. We clearly demonstrate that the neutrino mass matrix, which arises from the breaking of the electroweak symmetry and lepton-number violations, cannot explain the neutrino data due to the protection of $U(1)_{L_\mu - L_\tau}$ gauge invariance. In order to obtain a realistic neutrino mass matrix, we have to rely on other pieces

of Yukawa interactions, which can break the $U(1)$ symmetry. Concerning the magnitude of v_Δ, according to the electroweak symmetry breaking, the electroweak ρ-parameter at the tree-level can be written as [45]:

$$\rho = \frac{m_W^2}{m_Z^2 c_{\theta_W}^2} = \frac{1 + 2v_\Delta^2/v_H^2}{1 + 4v_\Delta^2/v_H^2}\,. \tag{4}$$

Taking the current precision measurement for ρ-parameter within 2σ errors, the VEV of Δ has to be less than 3.4 GeV.

In addition to Eq. (2), the gauge invariant Yukawa couplings to the Higgs and $S^{(\prime)}$ are given by:

$$\begin{aligned}
-\mathcal{L}_Y = {} & Y_\ell \bar{L}_\ell H \ell_R + y_\mu \bar{L}_{5L} H \mu_R + y_\tau \bar{L}_{4L} H \tau_R + y'_\mu \bar{L}_\mu L_{4R} S + y'_\tau \bar{L}_\tau L_{5R} S^\dagger \\
& + y_e \bar{L}_e L_{4R} S' + y'_e \bar{L}_e L_{5R} S'^\dagger + y_S \bar{L}_{5L} L_{4R} S + y'_S \bar{L}_{4L} L_{5R} S^\dagger \\
& + m_{4L} \bar{L}_{4L} L_{4R} + m_{5L} \bar{L}_{5L} L_{5R} + m_{4\tau} \bar{L}_{4R} L_\tau + m_{5\mu} \bar{L}_{5R} L_\mu + H.c.\,,
\end{aligned} \tag{5}$$

where H is the SM Higgs doublet; only the first term is from the SM, and the other terms are the new Yukawa interactions. Although Eq. (5) can cause rich interesting phenomena for lepton-flavor physics, we only focus on neutrino physics in this work, and a detailed study on the flavor physics can be found in [34]. Based on the Yukawa interactions in Eq. (5), it is found that the new entries of the Majorana mass matrix can be induced from higher dimensional operators, where the Feynman diagrams are sketched in Fig. 1, and the associated gauge invariant dimension-5 and -6 operators can be formulated as:

$$\begin{aligned}
-\mathcal{L}_Y \supset {} & \frac{Y_{\mu 4} y'^*_\mu}{m_{4L}} L_\mu^T C \bar{\Delta} L_\mu S^\dagger + \frac{Y_{\tau 5} y'^*_\tau}{m_{5L}} L_\tau^T C \bar{\Delta} L_\tau S + \left(\frac{Y_{\mu 4} y_e^*}{m_{4L}} + \frac{y_e^* Y'_{45} m_{5\mu}}{m_{4L} m_{5L}} \right) \\
& \times L_e^T C \bar{\Delta} L_\mu S'^\dagger \\
& + \left(\frac{Y_{\tau 5} y'^*_e}{m_{5L}} + \frac{y'^*_e Y'_{45} m_{4\tau}}{m_{4L} m_{5L}} \right) L_e^T C \bar{\Delta} L_\tau S' + \frac{Y'_{45} (y_e y'_e)^*}{m_{4L} m_{5L}} L_e^T C \bar{\Delta} L_e S' S'^\dagger \\
& + \frac{y'^*_e Y'_{45} y'^*_\mu}{m_{4L} m_{5L}} L_e^T C \bar{\Delta} L_\mu S^\dagger S' + \frac{y_e^* Y'_{45} y'^*_\tau}{m_{4L} m_{5L}} L_e^T C \bar{\Delta} L_\tau S S'^\dagger + \frac{Y_{\mu 4} y'_S y'^*_\tau}{m_{4L} m_{5L}} L_\mu^T C \bar{\Delta} L_\tau S S^\dagger \\
& + \frac{Y_{\tau 5} y_S y'^*_\mu}{m_{4L} m_{5L}} L_\tau^T C \bar{\Delta} L_\mu S S^\dagger + \frac{(Y_{45} + Y'_{45}) y'^*_\tau y'^*_\mu}{m_{4L} m_{5L}} L_\mu^T C \bar{\Delta} L_\tau S S^\dagger \\
& + \frac{Y_{\mu 4} m_{4\tau}}{m_{4L}} L_\mu^T C \bar{\Delta} L_\tau + \frac{Y_{\tau 5} m_{5\mu}}{m_{5L}} L_\tau^T C \bar{\Delta} L_\mu + H.c.
\end{aligned} \tag{6}$$

with $\bar{\Delta} = i\tau_2 \Delta$. From the effective Lagrangian, when the $U(1)_{L_\mu - L_\tau}$ gauge symmetry is spontaneously broken by $\langle S \rangle = v_S/\sqrt{2}$ and $\langle S' \rangle = v_{S'}/\sqrt{2}$, the vanishing elements in Eq. (3) can be generated from Eq. (6) with $\langle \Delta \rangle = v_\Delta/\sqrt{2}$. We note that the dimension-6 operator $L_\mu^T C \bar{\Delta} \bar{\Delta}^\dagger \bar{\Delta} L_\tau$ has been dropped due to $v_\Delta \ll v_{S,S'}$. From Eq. (6), it can be seen that after electroweak symmetry breaking, the $m_{4\mu}$ and $m_{5\tau}$ effects can be combined with other terms as:

$$\begin{aligned}
& Y_{\mu 4} + \frac{m_{5\mu}}{m_{5L}} Y'_{45} \to \tilde{Y}_{\mu 4}\,, \\
& Y_{\tau 5} + \frac{m_{4\tau}}{m_{4L}} Y'_{45} \to \tilde{Y}_{\tau 5}\,,
\end{aligned}$$

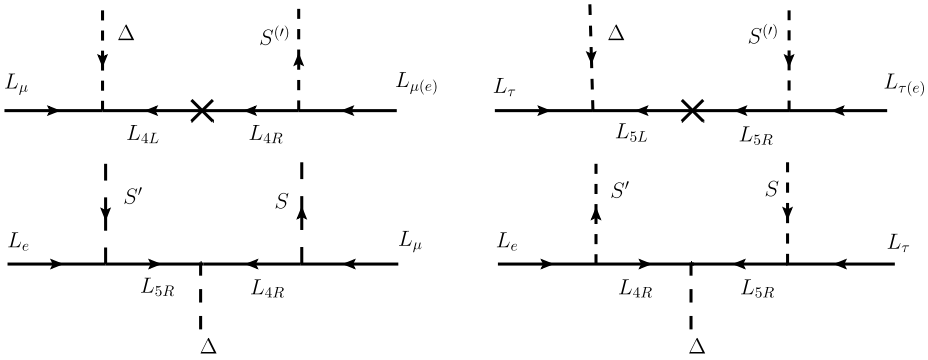

Fig. 1. Sketched Feynman diagrams for the Majorana neutrino mass matrix elements.

$$\frac{v_S^2}{2m_{4L}m_{5L}}y'_S y'^*_\tau + \frac{m_{4\tau}}{m_{4L}} \to \frac{v_S^2}{2m_{4L}m_{5L}}\tilde{y}'_S y'^*_\tau ,$$
$$\frac{v_S^2}{2m_{4L}m_{5L}}y_S y'^*_\mu + \frac{m_{5\mu}}{m_{5L}} \to \frac{v_S^2}{2m_{4L}m_{5L}}\tilde{y}_S y'^*_\mu . \tag{7}$$

Thus, to fit the neutrino masses, we need to take $m_{4\tau,5\mu} \ll m_{4L,5L}$.

Since the neutrino masses are generated by the spontaneous $U(1)_{L_\mu - L_\tau}$ symmetry breaking, we need to find the necessary conditions for vacuum stability. We thus write the gauge invariant scalar potential in this model as:

$$\begin{aligned}\mathcal{V} =& m_H^2 H^\dagger H + m_\Delta^2 \mathrm{Tr}[\Delta^\dagger\Delta] + m_{S'}^2 S'^\dagger S' + m_S^2 S^\dagger S + \mu_\Delta[H^T(i\tau_2)\Delta^\dagger H + \mathrm{h.c.}] \\ &+ \mu_S[S'S'S^\dagger + \mathrm{h.c.}] + \lambda_1|H^\dagger H|^2 + \lambda_2(\mathrm{Tr}[\Delta^\dagger\Delta])^2 + \lambda_3\mathrm{Tr}[(\Delta^\dagger\Delta)^2] + \lambda_4|S'^\dagger S'|^2 \\ &+ \lambda_5|S^\dagger S|^2 + \lambda_6(H^\dagger H)\mathrm{Tr}[\Delta^\dagger\Delta] + H^\dagger\left(\lambda_7\Delta\Delta^\dagger + \lambda_8\Delta^\dagger\Delta\right)H + \lambda_9(S'^\dagger S')(H^\dagger H) \\ &+ \lambda_{10}(S^\dagger S)(H^\dagger H) + \lambda_{11}(S'^\dagger S')\mathrm{Tr}[\Delta^\dagger\Delta] + \lambda_{12}(S^\dagger S)\mathrm{Tr}[\Delta^\dagger\Delta] + \lambda_{13}(S'^\dagger S')(S^\dagger S) .\end{aligned} \tag{8}$$

The VEVs of scalar fields are obtained by the minimal conditions $\partial\langle\mathcal{V}\rangle/\partial v_{H,S,S',\Delta} = 0$, and each condition can be expressed as:

$$\frac{\partial\langle\mathcal{V}\rangle}{\partial v_H} \simeq m_H^2 v_H + \lambda_1 v_H^3 + \frac{1}{2}\lambda_9 v_{S'}^2 v_H + \frac{1}{2}\lambda_{10} v_S^2 v_H \simeq 0, \tag{9}$$
$$\frac{\partial\langle\mathcal{V}\rangle}{\partial v_S} \simeq m_S^2 v_S + \frac{1}{\sqrt{2}}\mu_S v_{S'}^2 + \lambda_5 v_S^3 + \frac{1}{2}\lambda_{10} v_H^2 v_S + \frac{1}{2}\lambda_{13} v_{S'}^2 v_S \simeq 0, \tag{10}$$
$$\frac{\partial\langle\mathcal{V}\rangle}{\partial v_{S'}} \simeq m_{S'}^2 v_{S'} + \sqrt{2}\mu_S v_{S'} v_S + \lambda_4 v_{S'}^3 + \frac{1}{2}\lambda_9 v_H^2 v_{S'} + \frac{1}{2}\lambda_{13} v_S^2 v_{S'} \simeq 0, \tag{11}$$
$$\frac{\partial\langle\mathcal{V}\rangle}{\partial v_\Delta} \simeq m_\Delta^2 v_\Delta + \frac{1}{\sqrt{2}}\mu_\Delta v_H^2 + \frac{1}{2}(\lambda_6 + \lambda_7) v_H^2 v_\Delta + \frac{1}{2}\lambda_{11} v_{S'}^2 v_\Delta + \frac{1}{2}\lambda_{12} v_S^2 v_\Delta \simeq 0, \tag{12}$$

where we have ignored the v_Δ terms in the first three equations and the v_Δ^3 terms in the last equation due to $v_\Delta \ll v_{H,S,S'}$. In order to avoid the precision Higgs measurements, we can assume the mixing between H and $S(S')$ to be small, where the scalar mixing is discussed below; then, the VEV of H can be simplified as $v_H \approx \sqrt{-m_H^2/\lambda_1}$. If we further assume λ_{13} and μ_S

to be small, the VEVs of S and S' can be found as $v_S \approx \sqrt{-m_S^2/\lambda_5}$ and $v_{S'} \approx \sqrt{-m_{S'}^2/\lambda_4}$ with $m_{S,S'}^2 < 0$. The v_S and $v_{S'}$ are free parameters and their relation to the Z'-boson mass is given by $m_{Z'}^2 = g_{Z'}^2(4v_S^2 + v_{S'}^2)$; hence, their magnitudes can be taken as the electroweak scale. From Eq. (12), the VEV of Higgs triplet can be determined as [54]:

$$v_\Delta \simeq -\frac{1}{\sqrt{2}} \frac{\mu_\Delta v_H^2}{m_\Delta^2 + (\lambda_6 + \lambda_7)v_H^2/2 + \lambda_{11} v_{S'}^2/2 + \lambda_{12} v_S^2/2}\,. \tag{13}$$

Because $v_\Delta < 3.4$ GeV, in order to obtain the heavy Higgs triplet bosons, unlike the Higgs doublet and $S(S')$, m_Δ^2 has to be positive and must also dictate the masses of the Higgs triplet bosons. From Eq. (13), it can be seen that similar to the type-II seesaw model [44,45], the Higgs triplet VEV is directly related to the lepton-number soft breaking term.

We make a remark on the oblique parameter constraint. For the Higgs triplet, the mass difference between the Higgs triplet components is predominantly dictated by the oblique T-parameter, where the mass splitting between singly and doubly charged Higgs mass is bounded as $|m_{H^{\pm\pm}} - m_{H^{\pm(H^0)}}| \lesssim 50$ GeV [46–48]. Since our study does not directly relate to the mass splitting of the Higgs triplet, we can take $m_{H^{\pm\pm}} \approx m_{H^{\pm(H^0)}}$ to satisfy the constraint. Similarly, because the particle masses in $L_{4(5)}$ are taken to be the same, the vector-like leptons contributing to the T-parameter are small and can be neglected.

Although the involved new scalars do not directly affect the neutrino physics in this study, it is of interest to understand the limit from the current SM Higgs precision measurements. Thus, we briefly discuss the mixings among the SM Higgs and new scalar bosons in the following analysis. Since the mixing between the SM Higgs and the Higgs triplet is suppressed by the small VEV of the Higgs triplet field, therefore, we consider the situations in the SM Higgs and singlet scalars. Moreover, if we take $\lambda_{9,13} \ll 1$, the mixing between the SM Higgs and S' is suppressed and can be neglected. Thus, in order to show the constraint of the Higgs precision measurements, we only focus on the H–S mixing. Using the scalar potential in Eq. (8) and $H^T = (G^+, (v + \tilde{h} + iG^0)/\sqrt{2})$ and $S = (v_S + \tilde{s} + i\eta_S)/\sqrt{2}$, where G^+ and G^0 are the Nambu–Goldstone bosons in the SM, the squared mass matrix for the $\tilde{h}$ and $\tilde{s}$ scalar bosons can be obtained as:

$$\mathcal{L} \supset \frac{1}{2}\begin{pmatrix}\tilde{h}\\ \tilde{s}\end{pmatrix}^T \begin{pmatrix}\lambda_1 v^2 & \frac{\lambda_{10}}{2} v v_S \\ \frac{\lambda_{10}}{2} v v_S & \lambda_5 v_S^2\end{pmatrix}\begin{pmatrix}\tilde{h}\\ \tilde{s}\end{pmatrix}. \tag{14}$$

Using the 2×2 orthogonal matrix, written as:

$$\begin{pmatrix}h\\ s\end{pmatrix} = \begin{pmatrix}\cos\alpha & \sin\alpha \\ -\sin\alpha & \cos\alpha\end{pmatrix}\begin{pmatrix}\tilde{h}\\ \tilde{s}\end{pmatrix}, \tag{15}$$

the eigenvalues of the mass-square matrix and the mixing angle α can be obtained as:

$$\begin{aligned} m_{h,s}^2 &= \frac{\lambda_1 v^2 + \lambda_5 v_S^2}{2} \pm \frac{1}{2}\sqrt{\left(\lambda_1 v^2 - \lambda_5 v_S^2\right)^2 + \lambda_{10}^2 v^2 v_S^2}\,, \\ \sin 2\alpha &= \frac{\lambda_{10} v v_S}{m_h^2 - m_S^2}\,, \end{aligned} \tag{16}$$

where α is the mixing angle, and h is identified as the SM-like Higgs boson. It is clearly seen that in addition to the VEV of the Higgs field, the mixing effect of h and s is associated with the λ_{10} parameter and the VEV of S field.

Although there are several channels for the SM-like Higgs production and decays, the most accurate measurement in the LHC is the gluon-gluon fusion (ggF) Higgs production and the Higgs

diphoton decay, i.e. $pp(gg) \to h \to \gamma\gamma$. Thus, we only concentrate on the $h \to \gamma\gamma$ mode. For illustrating the influence of the new physics effects, we use the signal strength for $pp \to h \to \gamma\gamma$, defined as:

$$\mu_{\gamma\gamma} = \frac{\sigma(pp \to h)_{\rm SM+NP}}{\sigma(pp \to h)_{\rm SM}} \frac{BR(h \to \gamma\gamma)_{\rm SM+NP}}{BR(h \to \gamma\gamma)_{\rm SM}}\,, \tag{17}$$

where the ATLAS and CMS results using luminosities of 80 fb^{-1} and 35 fb^{-1} at $\sqrt{s} = 13$ TeV are given by $\mu_{ggF} = 0.97^{+0.15}_{-0.14}$ [49] and $\mu_{ggF} = 1.02^{+0.19}_{-0.18}$ [50], respectively. According to the current data, we can take $\delta\mu^{\rm NP}_{\gamma\gamma} = \mu_{\gamma\gamma} - 1 = \pm 15\%$ to constrain the new physics effect.

From Eq. (16), the SM Higgs couplings are modified by a factor of $\cos\alpha$; thus, we obtain $\sigma(pp \to h)_{\rm SM+NP} \simeq \cos^2\alpha \times \sigma(pp \to h)_{\rm SM}$. For the h decays, in addition to the SM channels, the h can also decay into the ss and $Z'Z'$ final states when kinematically allowed in this model. In order to include these two decay modes, we write the relevant interactions as:

$$\mathcal{L} \supset 4g^2_{Z'} v_S \sin\alpha h Z'_\mu Z'^\mu - \frac{1}{2} g_{hss} h s s\,, \tag{18}$$

where with $\lambda_1 \simeq (m_h/v)^2$ and $\lambda_5 \simeq (m_s/v_S)^2$, the effective coupling g_{hss} from the scalar potential can be obtained as:

$$\begin{aligned} g_{h\phi\phi} \simeq\ & 6\sin\alpha\cos\alpha\left(\frac{m_h^2}{v}\sin\alpha + \frac{m_s^2}{v_S}\cos\alpha\right) \\ & + \lambda_{10}(v\cos^3\alpha + v_S\sin^3\alpha - 2v_S\sin\alpha\cos^2\alpha - 2v\sin^2\alpha\cos\alpha)\,. \end{aligned} \tag{19}$$

Accordingly, the partial decay rates for the $h \to ss$ and $h \to Z'Z'$ processes can be formulated as:

$$\begin{aligned} \Gamma_{h\to Z'Z'} &= \frac{2g'^4 v_S^2 \sin^2\alpha}{\pi m_h}\sqrt{1 - \frac{4m^2_{Z'}}{m_h^2}}\left(2 + \frac{m_h^4}{4m^4_{Z'}}\left(1 - \frac{2m^2_{Z'}}{m_h^2}\right)^2\right), \\ \Gamma_{h\to ss} &= \frac{g^2_{hss}}{32\pi m_h}\sqrt{1 - \left(\frac{2m_s}{m_h}\right)^2}\,. \end{aligned} \tag{20}$$

As a result, the $\mu_{\gamma\gamma}$ signal strength in Eq. (17) can be obtained as:

$$\mu_{\gamma\gamma} = \cos^4\alpha \frac{\Gamma_h^{SM}}{\cos^2\alpha\Gamma_h^{SM} + \Gamma_{h\to ss} + \Gamma_{h\to Z'Z'}}\,, \tag{21}$$

where $\Gamma_h^{SM} \simeq 4.07$ MeV is the decay width of the SM Higgs [51]. Using Eq. (16) and $v_S = m_{Z'}/(\sqrt{5}g_{Z'})$, which arises from $v_S = v_{S'}$, we show $\delta\mu^{\rm NP}_{\gamma\gamma}$ as a function of λ_{10} in the left panel of Fig. 2, where $m_{Z'} = 0.2$ GeV and $g_{Z'} = 10^{-3}$ motivated from the muon $g-2$ are used. With $m_s = 10(200)$ GeV, the upper limit of λ_{10} can be $\sim 0.01(0.05)$, whereas the corresponding value of $\sin\alpha$ is $\sim 0.004(0.01)$. Since we focus on a light S-boson in the phenomenological analysis, the effects of the small mixing α angle can be neglected. In the considered parameter region, s and Z' mainly decay into $Z'Z'$ and $\bar{\nu}\nu$, respectively, it is of interest to see the constraint from the invisible Higgs decays, where the current upper limit of branching ratio (BR) is $BR(h \to$ invisible$) < 0.24$ [52,53]. Thus, we show $BR(h \to ss)$ (dotted), $BR(h \to Z'Z')$ (dashed), and $BR(h \to ss + Z'Z')$ (solid) as a function of λ_{10} in the right panel of Fig. 2. It can be clearly seen that the constraint from $\delta\mu^{\rm NP}_{\gamma\gamma}$ is stricter than that from the invisible Higgs decays.

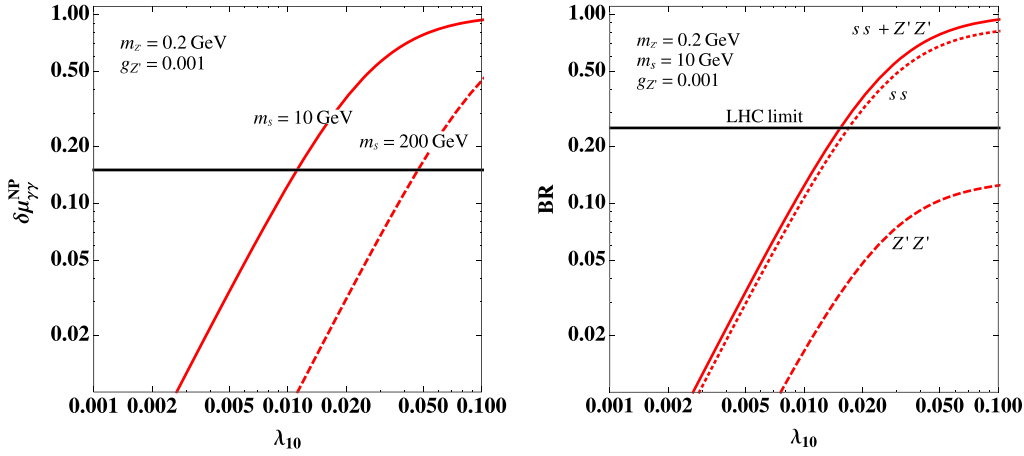

Fig. 2. Left: $\delta\mu^{\rm NP}_{\gamma\gamma}$ as a function of λ_{10} with $m_s = 200$ GeV (dashed) and $m_s = 20$ GeV (solid), where the taken values of the other parameters are shown on the plot. Right: BRs for the $h \to ss$ (dotted), $h \to Z'Z'$ (dashed), and $h \to ss + Z'Z'$ (solid) decays. The horizontal line denotes the experimental upper bound.

3. Charged lepton flavor mixing matrix

Since the PMNS matrix is related to the neutrino and charged-lepton flavor mixing matrices, before discussing the neutrino mass generation in this model, we first analyze the possibly sizable charged-lepton flavor mixing. As mentioned before, the active neutrino mass matrix is dictated by the Yukawa couplings in Eqs. (2) and (5), therefore, to explain the neutrino masses below the eV scale, most parameters have to be many orders of magnitude smaller than one. On the other hand, in order to have implications on the flavor physics, such as $h \to \mu\tau$ and $H^{--} \to \mu\tau$, we need some parameters to be of $O(10^{-2} - 10^{-1})$. In order to simplify the analysis on the charged-lepton flavor mixing, we thus ignore the small parameters, which are dictated by the neutrino masses, select the potentially sizable parameters, such as $y_{\mu,\tau}$, $y'_{\mu,\tau}$, and Y_{45}, and use these parameters to formulate the flavor mixing matrix. The reason to select these parameters will be clear in the later analysis.

The SM charged leptons and the introduced heavy leptons form a multiplet state in flavor space, denoted by $\ell'^T = (\boldsymbol{\ell}, \boldsymbol{\Psi}_\ell)$ with $\boldsymbol{\ell} = (e, \mu, \tau)$ and $\boldsymbol{\Psi}^T_\ell = (L_4, L_5)$. From Eq. (5), the 5×5 lepton mass matrix can be written as:

$$\bar{\ell}'_L M_{\ell'} \ell'_R = \left(\bar{\boldsymbol{\ell}}_L \,,\; \bar{\boldsymbol{\Psi}}_{\ell L} \right) \left(\begin{array}{c|c} \boldsymbol{m}_{\ell 3\times 3} & \boldsymbol{\delta m}_1 \\ \hline \boldsymbol{\delta m}_2^T & \boldsymbol{m}_L \end{array} \right)_{5\times 5} \left(\begin{array}{c} \boldsymbol{\ell}_R \\ \boldsymbol{\Psi}_{\ell R} \end{array} \right), \tag{22}$$

where $\mathrm{diag}\boldsymbol{m}_{\boldsymbol{\ell}} = (m_e, m_\mu, m_\tau)$, $m_f = v_H Y_f/\sqrt{2}$, $\mathrm{diag}\boldsymbol{m}_L = (m_{4L}, m_{5L})$, and $\boldsymbol{\delta m}_{1,2}$ are given by:

$$\boldsymbol{\delta m}_1^T = \begin{pmatrix} 0\,, & \frac{v_S y'_\mu}{\sqrt{2}}\,, & 0 \\ 0\,, & 0\,, & \frac{v_S y'_\tau}{\sqrt{2}} \end{pmatrix}, \quad \boldsymbol{\delta m}_2^T = \begin{pmatrix} 0\,, & 0\,, & \frac{v_H y_\tau}{\sqrt{2}} \\ 0\,, & \frac{v_H y_\mu}{\sqrt{2}}\,, & 0 \end{pmatrix}. \tag{23}$$

The mass matrix $M_{\ell'}$ in Eq. (22) can be diagonalized by the unitary matrices $U_\ell^{R,L}$ through $M_{\ell'}^{\rm dia} = U_\ell^L M_{\ell'} U_\ell^{R^\dagger}$. Due to $v_{H,S} \ll m_{4L,5L}$, we can expand the flavor mixing effects in terms of $v_{H,S}/m_{4L,5L}$; therefore, the 5×5 flvaor mixing matrices can be simplified as:

$$U_\ell^\chi \approx \left(\begin{array}{c|c} \mathbb{1}_{3\times 3} & -\boldsymbol{\epsilon}_\chi \\ \hline \boldsymbol{\epsilon}_\chi^\dagger & \mathbb{1}_{2\times 2} \end{array}\right)_{5\times 5}, \tag{24}$$

where we only retain the leading contributions, and the effects, which are smaller than $\boldsymbol{\epsilon_\chi}$ with $\chi = R, L$, have been dropped, such as $\boldsymbol{\epsilon}_\chi^\dagger \boldsymbol{\epsilon}_\chi$, $\boldsymbol{m}_\ell \boldsymbol{\delta m}_{1,2}/\boldsymbol{m}_L^2$, etc. The explicit expressions of $\boldsymbol{\epsilon_\chi}$ are given as:

$$\boldsymbol{\epsilon}_{\boldsymbol{L}}^\dagger = \begin{pmatrix} 0, & \frac{v_S y'_\mu}{\sqrt{2} m_{4L}}, & 0 \\ 0, & 0, & \frac{v_S y'_\tau}{\sqrt{2} m_{5L}} \end{pmatrix}, \quad \boldsymbol{\epsilon}_{\boldsymbol{R}}^\dagger = \begin{pmatrix} 0, & 0, & \frac{v_H y_\tau}{\sqrt{2} m_{4L}} \\ 0, & \frac{v_H y'_\mu}{\sqrt{2} m_{5L}}, & 0 \end{pmatrix}, \tag{25}$$

where the Yukawa couplings $y_{\mu,\tau}$ and $y'_{\mu,\tau}$ are taken as real numbers. If we use $v_S \approx 100$ GeV, $m_{4L} \approx m_{5L} \approx 1000$ GeV, and $y^{(\prime)}_{\mu(\tau)} \sim 0.1$, the off-diagonal mixing matrix elements of U_ℓ^χ are of $O(10^{-2})$. Comparing with the PMNS matrix, where the minimal element is $\mathbf{U}_{13} \sim 0.14$ and is one oder of magnitude larger than $(U_\ell^\chi)_{ij}$ with $i \neq j$, we can approximate the PMNS matrix to be $\mathbf{U} \equiv U_\nu^L U_\ell^{L\dagger} \approx U_\nu^L$. That is, in this leading order approximation, we can use the PMNS matrix to diagonalize the induced neutrino mass matrix.

After rotating the lepton weak states to physical states based on the U_ℓ^R and U_ℓ^L, the Yukawa couplings of the SM Higgs to the charged leptons are expressed as:

$$-\mathcal{L}_h = \left(\bar{\boldsymbol{\ell}}_{\boldsymbol{L}}, \bar{\boldsymbol{\Psi}}_{\ell L}\right) U_\ell^L \left(\begin{array}{c|c} \boldsymbol{m_\ell}_{3\times 3} & 0 \\ \hline \boldsymbol{\delta m_2^T} & 0 \end{array}\right) U_\ell^{R^\dagger} \begin{pmatrix} \boldsymbol{\ell_R} \\ \boldsymbol{\Psi}_{\ell R} \end{pmatrix} \frac{h}{v_H}, \tag{26}$$

where we still use $\boldsymbol{\ell}$ and $\boldsymbol{\Psi}_\ell^T$ to represent the charged leptons. As a result, the SM Higgs Yukawa couplings to the light charged leptons can be found as:

$$-\mathcal{L}_h \supset \frac{m_\ell}{v_H} \bar{\ell}_L \ell_R h - \frac{v_S y'_\mu y_\tau}{2 m_{4L}} \bar{\mu}_L \tau_R h - \frac{v_S y'_\tau y_\mu}{2 m_{5L}} \bar{\tau}_L \mu_R h + H.c. \tag{27}$$

The second and third terms can lead to the $h \to \mu\tau$ decay.

4. Majorana neutrino mass matrix and FGM patterns

In this section, we discuss the neutrino mass matrix and some phenomenology in our model. When we write the symmetric Majorana neutrino mass matrix as:

$$M^\nu = \begin{pmatrix} m_{ee} & m_{e\mu} & m_{e\tau} \\ m_{e\mu} & m_{\mu\mu} & m_{\mu\tau} \\ m_{e\tau} & m_{\mu\tau} & m_{\tau\tau} \end{pmatrix}, \tag{28}$$

from the Yukawa couplings in Eqs. (2) and (6), each matrix element can then be expressed as:

$$m_{ee} = \frac{Y_{ee} v_\Delta}{\sqrt{2}} + \frac{Y'_{45} y_e^* y_e'^* v_{S'}^2 v_\Delta}{2\sqrt{2} m_{4L} m_{5L}}, \; m_{e\mu} = \frac{y_e^* Y_{\mu 4} v_{S'} v_\Delta}{\sqrt{2} m_{4L}} + \frac{Y'_{45} y_e'^* y_\mu'^*}{2\sqrt{2}} \frac{v_S v_{S'} v_\Delta}{m_{4L} m_{5L}} + \frac{Y'_{45} y_e^* m_{5\mu}}{2} \frac{v_{S'} v_\Delta}{m_{4L} m_{5L}},$$

$$m_{e\tau} = \frac{y'_e Y_{\tau 5} v_{S'} v_\Delta}{\sqrt{2} m_{5L}} + \frac{Y'_{45} y^*_e y'^*_\tau}{2\sqrt{2}} \frac{v_S v_{S'} v_\Delta}{m_{4L} m_{5L}} + \frac{Y'_{45} y'^*_e m_{4\tau}}{2} \frac{v_{S'} v_\Delta}{m_{4L} m_{5L}}\,,\ m_{\mu\mu} = \frac{Y_{\mu 4} y'^*_\mu v_S v_\Delta}{2 m_{4L}}\,,$$
$$m_{\mu\tau} = \frac{Y_{\mu\tau} v_\Delta}{\sqrt{2}} + \frac{Y_{\mu 4} m_{4\tau} v_\Delta}{\sqrt{2} m_{4L}} + \frac{Y_{\tau 5} m_{5\mu} v_\Delta}{\sqrt{2} m_{5L}} + \frac{\eta}{2\sqrt{2}} \frac{v_S^2 v_\Delta}{m_{4L} m_{5L}}\,,\ m_{\tau\tau} = \frac{Y_{\tau 5} y'^*_\tau v_S v_\Delta}{2 m_{5L}} \tag{29}$$

with $\eta = Y_{\mu 4} y'_S y'^*_\tau + Y_{\tau 5} y_S y'^*_\mu + (Y_{45} + Y'_{45}) y'^*_\tau y'^*_\mu$. Although the neutrino mass matrix comes from the dimension-4, -5, and -6 operators, since the involved free parameters are different, the matrix entries in Eq. (29) can be taken as the same order of magnitude with no particular hierarchy, unless there is a further indication. Due to the $U(1)_{L_\mu - L_\tau}$ gauge symmetry, the light charged-lepton mass matrix in the first term of Eq. (5) is diagonal. Although the other Yukawa interactions can induce off-diagonal elements, as shown earlier, these induced terms indeed are suppressed. If we neglect these small off-diagonal effects as a leading approximation, the Majorana neutrino mass matrix can be diagonalized by the PMNS matrix as $M^\nu_{\rm dia} = {\rm diag}(m_1, m_2, m_3) = {\rm diag}(|m_1| e^{-i\alpha_{13}}, |m_2| e^{-i\alpha_{23}}, |m_3|) = \mathbf{U}^T M^\nu \mathbf{U}$, where α_{13} and α_{23} are the Majorana CP violating phases, and the standard parametrization of PMNS matrix is given as [5]:

$$\mathbf{U} = \begin{pmatrix} c_{12}c_{13} & s_{12}c_{13} & s_{13}e^{-i\delta} \\ -s_{12}c_{23} - c_{12}s_{23}s_{13}e^{i\delta} & c_{12}c_{23} - s_{12}s_{23}s_{13}e^{i\delta} & s_{23}c_{13} \\ s_{12}s_{23} - c_{12}c_{23}s_{13}e^{i\delta} & -c_{12}s_{23} - s_{12}c_{23}s_{13}e^{i\delta} & c_{23}c_{13} \end{pmatrix} \tag{30}$$

with $s_{ij} \equiv \sin\theta_{ij}$, $c_{ij} \equiv \cos\theta_{ij}$, and δ being the Dirac CP violating phase.

From Eq. (28), there are six different complex matrix elements. After rotating three unphysical phases, we have nine independent parameters. Since neutrino oscillation experiments cannot observe the two Majorana CP phases, even we assume $\alpha_{13} = \alpha_{23} = 0$, there are seven free parameters. However, we only have six observables: $\Delta m^2_{21,31}$, $\sin^2\theta_{12,13,23}$, and Dirac CP phase δ; that is, we cannot determine all free parameters without further theoretical or experimental inputs. It has been suggested that a class of neutrino mass matrices may suffice to explain all neutrino experiments if the matrix textures have two independent zeroes [55]. The seven possible Frampton–Glashow–Marfatia (FGM) matrix patterns are classified as:

$$\mathbf{A}_1 : \begin{pmatrix} 0 & 0 & X \\ 0 & X & X \\ X & X & X \end{pmatrix}, \quad \mathbf{A}_2 : \begin{pmatrix} 0 & X & 0 \\ X & X & X \\ 0 & X & X \end{pmatrix}, \quad \mathbf{B}_1 : \begin{pmatrix} X & X & 0 \\ X & 0 & X \\ 0 & X & X \end{pmatrix},$$
$$\mathbf{B}_2 : \begin{pmatrix} X & 0 & X \\ 0 & X & X \\ X & X & 0 \end{pmatrix},$$
$$\mathbf{B}_3 : \begin{pmatrix} X & 0 & X \\ 0 & 0 & X \\ X & X & X \end{pmatrix}, \quad \mathbf{B}_4 : \begin{pmatrix} X & X & 0 \\ X & X & X \\ 0 & X & 0 \end{pmatrix}, \quad \mathbf{C} : \begin{pmatrix} X & X & X \\ X & 0 & X \\ X & X & 0 \end{pmatrix}, \tag{31}$$

where the symbol X denotes a nonzero texture. A detailed study with two-zero textures can be found in [58–60]. In order to simplify the analysis, we thus employ the FGM patterns as the theoretical inputs.

As mentioned earlier, the neutrino mass order is still uncertain, i.e. $|m_1| < |m_2| < |m_3|$ or $|m_3| < |m_1| < |m_2|$ is allowed. With an FGM pattern, it helps understand what form of a neutrino mass matrix can lead to a specific mass order. According to the study referenced in [61], by taking the neutrino data with 1σ errors, the NO spectrum could be achieved by the patterns $\mathbf{A}_{1,2}$

Table 2
Vanishing Yukawa (VY) couplings to determine the FGM two-zero textures in the model.

Pattern	$\mathbf{A}_1$	$\mathbf{A}_2$	$\mathbf{B}_1$	$\mathbf{B}_2$
VY	$(Y_{ee},\ Y'_{45},\ y_e)\approx 0$	$(Y_{ee},\ Y'_{45},\ y'_e)\approx 0$	$(y'_e,\ Y'_{45},\ y'_\mu)\approx 0$	$(y_e,\ Y'_{45},\ Y_{\tau 5})\approx 0$
Pattern	$\mathbf{B}_3$	$\mathbf{B}_4$	$\mathbf{C}$	
VY	$(y'_e,\ y_e,\ Y_{\mu 4})\approx 0$	$(y_e,\ Y_{\tau 5},\ m_{4\tau})\approx 0$	$(Y_{\mu 4},\ Y_{\tau 5})\approx 0$	

and $\mathbf{B}_{1,2,3,4}$, while the IO could be achieved by the patterns $\mathbf{B}_{1,3}$ and $\mathbf{C}$. Accordingly, it is of interest to see how the matrix elements of Eq. (29) in our model connect to those of a specific FGM matrix. It is found that when some Yukawa couplings are required to vanish, a definite FGM matrix pattern can then be achieved. We show the vanishing Yukawa couplings for the corresponding FGM matrix in Table 2. It is worth mentioning that a powerful FGM matrix pattern can also predict the absolute values of neutrino masses and Majorana CP-phases, which so far have not yet been observed in experiments. From the zero textures $M^\nu_{ij} = M^\nu_{kl} = 0$ $(ij \neq kl)$, the neutrino mass ratios and Majorana CP phases can be obtained as [58]:

$$\begin{aligned}
\frac{|m_1|}{|m_3|} &= \left| \frac{U_{i3}U_{j3}U_{k2}U_{l2} - U_{i2}U_{j2}U_{k3}U_{l3}}{U_{i2}U_{j2}U_{k1}U_{l1} - U_{i1}U_{j1}U_{k2}U_{l2}} \right| , \\
\frac{|m_2|}{|m_3|} &= \left| \frac{U_{i1}U_{j1}U_{k3}U_{l3} - U_{i3}U_{j3}U_{k1}U_{l1}}{U_{i2}U_{j2}U_{k1}U_{l1} - U_{i1}U_{j1}U_{k2}U_{l2}} \right| \\
\alpha_{13} &= \arg\left[\frac{U_{i3}U_{j3}U_{k2}U_{l2} - U_{i2}U_{j2}U_{k3}U_{l3}}{U_{i2}U_{j2}U_{k1}U_{l1} - U_{i1}U_{j1}U_{k2}U_{l2}} \right] , \\
\alpha_{23} &= \arg\left[\frac{U_{i1}U_{j1}U_{k3}U_{l3} - U_{i3}U_{j3}U_{k1}U_{l1}}{U_{i2}U_{j2}U_{k1}U_{l1} - U_{i1}U_{j1}U_{k2}U_{l2}} \right] .
\end{aligned} \tag{32}$$

The values of the neutrino mass ratios and CP phases for each pattern with two benchmark inputs are shown in Table 3, where in addition to the taken values of $\sin^2\theta_{12} = 0.304$ and $\sin^2\theta_{13} = 0.0219$, the values inside brackets correspond to two different inputs: for the left value, we fix $\delta = 1.5\pi$ and $\sin^2\theta_{23} = 0.5$; for the right, $\delta = 1.59205\pi$ and $\sin^2\theta_{23} = 0.4515$ are used. From the results, it can be seen that the patterns $\mathbf{A_1}$ and $\mathbf{A_2}$ prefer the normal hierarchy, and the patter $\mathbf{C}$ shows the inverted hierarchy and degenerate case. The mass ordering in patterns $\mathbf{B_{1-4}}$ depends on the taken parameters. For illustration, in the following analysis, we focus the detailed analysis on the patterns $\mathbf{A}_1$ and $\mathbf{C}$.

5. Numerical analysis and other phenomena of interest

5.1. Explain neutrino data and predict the absolute neutrino masses

Since our purpose is not to examine all FGM patterns, in the following numerical analysis, we take $\mathbf{A}_1$ and $\mathbf{C}$ as the representatives of the NO and IO mass spectra, respectively. To determine the non-vanishing entries of the neutrino mass matrix and $|m_i|$, we scan the parameters with the neutrino data at the 1σ level. Due to large experimental uncertainty, the Dirac CP phase is taken from a global data analysis using an χ^2 method [64], in which the result in the 1σ region is $\delta/\pi = (1.18, 1.61)$ for NO and $\delta/\pi = (1.12, 1.62)$ for IO. Combining the experimental inputs with two independent zero textures, we basically have eight known inputs; thus, we can completely constrain the four non-vanishing complex entries of $\mathbf{A}_1$ and $\mathbf{C}$.

Table 3
Mass ratios and Majorana CP phases of each FGM pattern with some benchmark inputs, where in addition to the taken values of $\sin^2\theta_{12}=0.304$ and $\sin^2\theta_{13}=0.0219$, the values inside brackets correspond to two different inputs: for the left value, we fix $\delta=1.5\pi$ and $\sin^2\theta_{23}=0.5$; for the right, $\delta=1.59205\pi$ and $\sin^2\theta_{23}=0.4515$ are taken.

	mass relation	CP-violating phases
$\mathbf{A}_1$	$\frac{\lvert m_1\rvert}{\lvert m_3\rvert}\simeq(0.10,\,0.087)$, $\frac{\lvert m_2\rvert}{\lvert m_3\rvert}\simeq(0.23,\,0.22)$	$\alpha_{13}\simeq(0.43\pi,\,0.33\pi)$, $\alpha_{23}\simeq(-0.47\pi,\,-0.56\pi)$
$\mathbf{A}_2$	$\frac{\lvert m_1\rvert}{\lvert m_3\rvert}\simeq(0.10,\,0.12)$, $\frac{\lvert m_2\rvert}{\lvert m_3\rvert}\simeq(0.23,\,0.25)$	$\alpha_{13}\simeq(-0.43\pi,\,-0.53\pi)$, $\alpha_{23}\simeq(0.47\pi,\,0.38\pi)$
$\mathbf{B}_1$	$\frac{\lvert m_1\rvert}{\lvert m_3\rvert}\simeq(1.0,\,0.95)$, $\frac{\lvert m_2\rvert}{\lvert m_3\rvert}\simeq(1.0,\,0.74)$	$\alpha_{13}\simeq(1.0\pi,\,-0.98\pi)$, $\alpha_{23}\simeq(-1.0\pi,\,-0.99\pi)$
$\mathbf{B}_2$	$\frac{\lvert m_1\rvert}{\lvert m_3\rvert}\simeq(1.0,\,1.1)$, $\frac{\lvert m_2\rvert}{\lvert m_3\rvert}\simeq(1.0,\,1.3)$	$\alpha_{13}\simeq(-1.0\pi,\,-0.98\pi)$, $\alpha_{23}\simeq(1.0\pi,\,-0.99\pi)$
$\mathbf{B}_3$	$\frac{\lvert m_1\rvert}{\lvert m_3\rvert}\simeq(1.0,\,0.73)$, $\frac{\lvert m_2\rvert}{\lvert m_3\rvert}\simeq(1.0,\,0.87)$	$\alpha_{13}\simeq(-1.0\pi,\,0.98\pi)$, $\alpha_{23}\simeq(-1.0\pi,\,-1.0\pi)$
$\mathbf{B}_4$	$\frac{\lvert m_1\rvert}{\lvert m_3\rvert}\simeq(1.0,\,1.4)$, $\frac{\lvert m_2\rvert}{\lvert m_3\rvert}\simeq(1.0,\,1.1)$	$\alpha_{13}\simeq(1.0\pi,\,0.98\pi)$, $\alpha_{23}\simeq(1.0\pi,\,-1.0\pi)$
$\mathbf{C}$	$\frac{\lvert m_1\rvert}{\lvert m_3\rvert}\simeq(1.0,\,1.19)$, $\frac{\lvert m_2\rvert}{\lvert m_3\rvert}\simeq(1.0,\,1.2)$	$\alpha_{13}\simeq(1.0\pi,\,0.70\pi)$, $\alpha_{23}\simeq(1.0\pi,\,-0.89\pi)$

Using the relation $M^\nu=\mathbf{U}^*M^\nu_{\rm dia}\mathbf{U}^\dagger$ and the zero textures in M^ν, the mass relations in $\mathbf{A}_1$ can be expressed as:

$$m_1^*=\frac{U_{13}}{U_{11}}\left(\frac{U_{12}U_{23}-U_{13}U_{22}}{U_{11}U_{22}-U_{12}U_{21}}\right)m_3^*,$$
$$m_2^*=-\frac{U_{13}}{U_{12}}\left(\frac{U_{11}U_{23}-U_{13}U_{21}}{U_{11}U_{22}-U_{12}U_{21}}\right)m_3^*, \tag{33}$$

while in $\mathbf{C}$, they are:

$$m_1^*=\frac{U_{22}^2U_{33}^2-U_{23}^2U_{32}^2}{U_{21}^2U_{32}^2-U_{22}^2U_{31}^2}m_3^*,$$
$$m_2^*=-\frac{U_{21}^2U_{33}^2-U_{23}^2U_{31}^2}{U_{21}^2U_{32}^2-U_{22}^2U_{31}^2}m_3^*, \tag{34}$$

where the m_ks values in general are complex; however, there are only two independent phases among $m_{1,2,3}$. With the chosen Majorana phases, such as $m_1=|m_1|e^{-i\alpha_{13}}$ and $m_2=|m_2|e^{-i\alpha_{23}}$, we obtain the relations

$$\alpha_{13}=\arg\left[\frac{U_{13}}{U_{11}}\left(\frac{U_{12}U_{23}-U_{13}U_{22}}{U_{11}U_{22}-U_{12}U_{21}}\right)\right],\quad \alpha_{23}=\arg\left[-\frac{U_{13}}{U_{12}}\left(\frac{U_{11}U_{23}-U_{13}U_{21}}{U_{11}U_{22}-U_{12}U_{21}}\right)\right] \tag{35}$$

for the $\mathbf{A}_1$ case, and

$$\alpha_{13}=\arg\left[\frac{U_{22}^2U_{33}^2-U_{23}^2U_{32}^2}{U_{21}^2U_{32}^2-U_{22}^2U_{31}^2}\right],\quad \alpha_{23}=\arg\left[-\frac{U_{21}^2U_{33}^2-U_{23}^2U_{31}^2}{U_{21}^2U_{32}^2-U_{22}^2U_{31}^2}\right] \tag{36}$$

for the $\mathbf{C}$ case. If we take the central values of measured $\theta_{12,13}$ in Eq. (1), $\sin^2\theta_{23}\approx0.50$, and $\delta\approx1.5\pi$, we can easily obtain:

$$\mathbf{A}_1:\begin{cases}|m_1|/|m_3|\approx0.230\,,\\ |m_2|/|m_3|\approx0.102\,,\\ |m_2|^2-|m_1|^2\approx0.029|m_3|^2\,,\\ \alpha_{13}\approx0.430\pi\,,\\ \alpha_{23}\approx-0.469\pi\,.\end{cases} \tag{37}$$

However, it is found that the pattern **C** is very sensitive to the values of the mixing angles and CP phase δ when Δm^2_{21} and Δm^2_{32} are required to fit the data within 1σ errors. If $\sin^2\theta_{23} \approx 0.4515$ and $\delta \approx 1.59205\pi$ are taken, we obtain:

$$\mathbf{C}: \begin{cases} |m_1|/|m_3| \approx 1.19\,, \\ |m_2|/|m_3| \approx 1.20\,, \\ |m_2|^2 - |m_1|^2 \approx 0.0130|m_3|^2\,, \\ \alpha_{13} \approx -0.705\pi\,, \\ \alpha_{23} \approx 0.887\pi\,. \end{cases} \tag{38}$$

Accordingly, if we further take $\Delta m^2_{21} \approx 7.53 \times 10^{-5}\ \text{eV}^2$, the values of $|m_i|$ and Δm^2_{23} can be determined as:

$$\mathbf{A}_1: \begin{cases} |m_1| \approx 5.5 \times 10^{-3}\ \text{eV}\,, \\ |m_2| \approx 1.03 \times 10^{-2}\ \text{eV}\,, \\ |m_3| \approx 5.06 \times 10^{-2}\ \text{eV}\,, \\ \Delta m^2_{32} \approx 2.45 \times 10^{-3}\ \text{eV}^2\,; \end{cases} \quad \mathbf{C}: \begin{cases} |m_3| \approx 7.60 \times 10^{-2}\ \text{eV}\,, \\ |m_1| \approx 9.07 \times 10^{-2}\ \text{eV}\,, \\ |m_2| \approx 9.11 \times 10^{-2}\ \text{eV}\,, \\ \Delta m^2_{23} \approx 2.53 \times 10^{-3}\ \text{eV}^2\,. \end{cases} \tag{39}$$

From above analysis, $\mathbf{A}_1$ and **C** can fit the neutrino data for the NO and IO mass spectra at the 1σ level, respectively. However, if we compare the results with the cosmological limit on the sum of neutrino masses, which is given as:

$$\sum_\nu m_\nu < (0.12, 0.17)\ \text{eV}\,, \tag{40}$$

([62], [63]) it can be found that the resulting $\sum_j |m_j|$ in $\mathbf{A}_1$ can satisfy the upper bound while that in **C** is higher than the limit. In order to determine whether the tension with the cosmological neutrino mass bound can be relaxed when the ranges of the experimental measurements are extended, we adopt neutrino data up to the 3σ level instead of those at the 1σ level for **C**. In the numerical analysis, we generate 5×10^8 sampling points by randomly selecting the experimental values of $s_{12,23,13}$ and δ within $\{1\sigma, 2\sigma, 3\sigma\}$ errors and the values of m_1 in the range of $[0.01, 0.17]$ eV; then, m_2 and m_3 are obtained via Eq. (34). In the end, the number of output points, which can fit the $\Delta m^2_{21,23}$ data in the $\{1\sigma, 2\sigma, 3\sigma\}$ range, is $\{552, 3004, 3467\}$. The obtained Dirac CP phase δ and $\sum_j |m_j|$ are shown in Fig. 3, where the dots in black, red and blue denote the results with 1σ, 2σ and 3σ errors, respectively. From the figure, it can be clearly seen that $\sum_j |m_j|$ in **C** is excluded even at the 3σ level if we adopt the bound from the cosmological measurements $\sum_\nu m_\nu < 0.12$ eV while it can still satisfy the bound at the 2σ level if we adopt the upper limit of 0.17 eV.

Since the uncertainties of $\sin^2\theta_{23}$ and Δm^2_{32} in Eq. (1) correspond to a 68% confidence level (CL), and the pattern **C** cannot fit the data within 1σ errors, in the remaining part of the paper, we only use the pattern $\mathbf{A}_1$ to show the constraints for the relevant Yukawa couplings. From the mass diagonal relation $M^\nu_{\ell\ell'} = (U_{\ell k} U_{\ell' k})^* m_k$, when the PMNS matrix entries and m_k are known, $M^\nu_{\ell\ell'}$ can then be determined. Thus, the correlation between δ and $|m_j|$ in $\mathbf{A}_1$ is shown in Fig. 4(a), where the neutrino data within 1σ error have been included. From the plot, it can be seen that each $|m_i|$ narrowly spreads around the value of Eq. (39). In the plot, we also show the effective Majorana neutrino mass $\langle m_{\beta\beta}\rangle$, which is related to the neutrinoless double-beta ($0\nu\beta\beta$) decay rate and is defined by [21]:

$$\langle m_{\beta\beta}\rangle = |\sum_k U^2_{ek} m_k|\,, \tag{41}$$

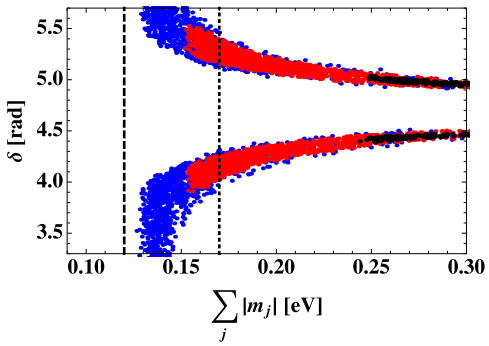

Fig. 3. Scatter plot for the Dirac CP phase and $\sum_j |m_j|$, where the dots in black, red, and blue denote the neutrino data with 1σ, 2σ, and 3σ errors, respectively. The dashed (dotted) line denote the cosmological neutrino mass bound 0.12(0.17) eV.

where a 90% CL upper limit of $\langle m_{\beta\beta}\rangle < 0.061 - 0.165$ eV was obtained by the KamLAND-Zen collaboration [65]. Our result of $\langle m_{\beta\beta}\rangle \approx (0.34, 2.3) \times 10^{-2}$ eV clearly satisfies the bound. According the results, the allowed ranges of $|m_{ij}|$ as a correlation of $|m_{\tau\tau}|$ are shown in Fig. 4(b), where we scan the parameters using 10^7 sampling points to fit the neutrino data, and $|m_1| \in [0.001, 0.1]$ eV is taken. As a result, the obtained ranges of m_{ij} in $\mathbf{A}_1$ are given as:

$$\begin{aligned} m_{e\tau} &= (0.99, 1.11) \times 10^{-2}\,\text{eV}\,, \quad m_{\mu\mu} = (2.5, 3.0) \times 10^{-2}\,\text{eV}\,, \\ m_{\mu\tau} &= (2.2, 2.4) \times 10^{-2}\,\text{eV}\,, \quad m_{\tau\tau} = (2.4, 2.8) \times 10^{-2}\,\text{eV}\,, \end{aligned} \tag{42}$$

where m_{ee} and $m_{e\mu}$ are zero in neutrino mass pattern $\mathbf{A}_1$. In addition, the correlation between the Dirac phase δ and Majorana phase $\alpha_{13}[\alpha_{23}]$ are shown in Fig. 4(c)[(d)].

5.2. Limits of Yukawa couplings and the $h \to \mu\tau$ decay

Based on the results obtained above, we now discuss the limits on the introduced Yukawa couplings shown in Eqs. (2) and (5). To simplify the analysis, we take $m_{4L} \approx m_{5L} \equiv m_L$ and $v_S \approx v_{S'} \equiv v_X$, and define the parameters as:

$$a_L = \frac{y'^*_\tau y^*_\mu v_X}{2m_L}\,, \quad a_R = \frac{y'_\mu y_\tau v_X}{2m_L}\,, \quad \xi^{(\prime)}_{ab} = \frac{Y^{(\prime)}_{ab} v_\Delta}{\sqrt{2}}\,. \tag{43}$$

The parameters $a_{R,L}$ can lead to the Higgs lepton-flavor violating $h \to \mu\tau$ decay, where the associated interactions from Eq. (27) are expressed as [56,57]:

$$\mathcal{L}_{h\tau\mu} = h\bar{\mu}(a_R P_R + a_L P_L)\tau + H.c. \tag{44}$$

The BR for $h \to \tau\mu$ can be obtained as:

$$BR(h \to \mu\tau) = \frac{|a_L|^2 + |a_R|^2}{8\pi\Gamma_h} m_h\,. \tag{45}$$

With $m_h \approx 125$ GeV and $\Gamma_h \approx 4.21$ MeV, the limit on $a_{L,R}$ can be obtained as

$$\sqrt{|a_L|^2 + |a_R|^2} \approx 1.56 \times 10^{-3} \sqrt{\frac{BR(h \to \tau\mu)}{2.5 \times 10^{-3}}}\,, \tag{46}$$

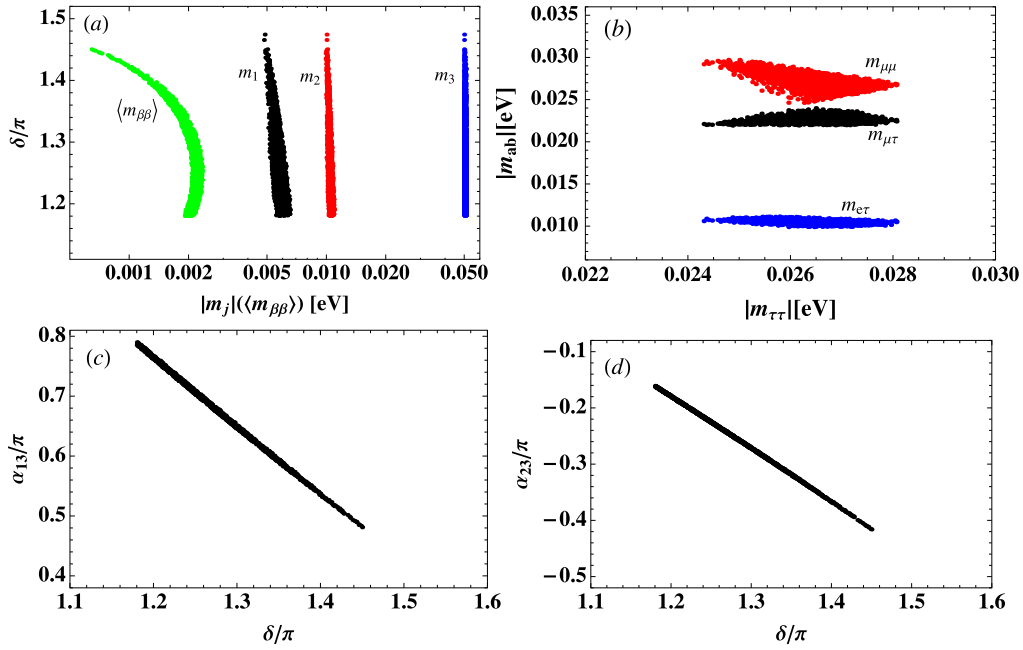

Fig. 4. (a) Predicted $|m_j|$ and effective Majorana neutrino mass for the $0\nu\beta\beta$ decay; (b) allowed ranges for $|m_{ij}|$ as a correlation of $|m_{\tau\tau}|$; (c)[(d)] correlation between Dirac phase δ and Majorana phase $\alpha_{13}[\alpha_{23}]$, where FGM pattern $\mathbf{A}_1$ is applied, and neutrino data within 1σ errors are taken.

where $BR(h \to \mu\tau)$ can be taken from the experimental data, and the current upper limits from ATLAS and CMS are 1.43% [66] and 0.25% [67,68], respectively.

Using $Y_{ee} \approx Y'_{45} \approx y_e \approx 0$ in $\mathbf{A}_1$, the neutrino mass matrix entries in Eq. (29) are formed as:

$$
\begin{aligned}
& m_{e\tau} = \frac{y'_e v_X}{m_L}\xi_{\tau 5}\,, \quad m_{\mu\mu} = \frac{\sqrt{2}}{y^*_\tau}a^*_R\xi_{\mu 4}\,, \quad m_{\tau\tau} = \frac{\sqrt{2}}{y^*_\mu}a_L\xi_{\tau 5}\,, \\
& m_{\mu\tau} = \xi_{\mu\tau} + \left(\frac{m_{4\tau}}{m_L} + \frac{y'_S}{y^*_\mu}\frac{v_X}{m_L}a_L\right)\xi_{\mu 4} \\
& \quad + \left(\frac{m_{5\mu}}{m_L} + \frac{y_S}{y^*_\tau}\frac{v_X}{m_L}a^*_R\right)\xi_{\tau 5} + \frac{2}{y^*_\tau y^*_\mu}a_L a^*_R(\xi_{45} + \xi'_{45})\,.
\end{aligned}
\tag{47}
$$

In order to get sizable $BR(h \to \mu\tau)$ and ξ_{45}, we find that $|a_L| \ll |a_R|$ or $|a_R| \ll |a_L|$ has to be satisfied. According to Eq. (42), if we take $|m_{\mu\mu}| \approx |m_{\tau\tau}| \approx 2.7 \times 10^{-2}$ eV, $|m_{e\tau}| \approx 10^{-2}$ eV, $|m_{\mu\tau}| \approx 2.3 \times 10^{-2}$ eV, $|a_{R(L)}| \approx 10^{-3}(10^{-8})$, $v_X \approx 100$ GeV, and $m_L \approx 1000$ GeV, we can obtain $BR(h \to \mu\tau) \approx 1.2 \times 10^{-3}$, and the magnitudes of parameters are obtained as:

$$
\begin{aligned}
& |y'_e\xi_{\tau 5}| \approx 1.0 \times 10^{-10}\,\text{GeV}\,, \quad \left|\frac{\xi_{\mu 4}}{y_\tau}\right| \approx 1.9 \times 10^{-8}\,\text{GeV}\,, \\
& \left|\frac{\xi_{\tau 5}}{y_\mu}\right| \approx 1.9 \times 10^{-3}\,\text{GeV}\,, \quad |\xi_{\mu\tau}| \approx \left|2.3 - \frac{2\xi_{45}}{y^*_\mu y^*_\tau}\right| \times 10^{-11}\,\text{GeV}\,,
\end{aligned}
\tag{48}
$$

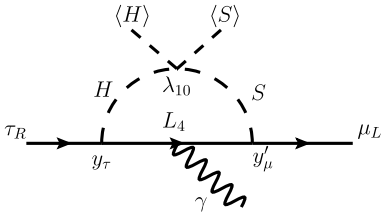

Fig. 5. Sketched Feynman diagram for $\tau \to \mu\gamma$.

where the second and third terms in $m_{\mu\tau}$ have been ignored due to $y_S, y'_S, m_{4\tau,5\mu}/m_L \ll 1$. With $y_\mu \approx y_\tau \approx 0.1$, the Higgs triplet Yukawa couplings then have the hierarchy $Y_{\mu\tau} \ll Y_{\mu 4} \ll Y_{\tau 5} \ll Y_{45}$; that is, we cannot avoid fine-tuning the Yukawa couplings to explain the neutrino data in this model.

According to above analysis, we see that the Yukawa couplings, which are not highly suppressed by the neutrino masses, are only y_μ, y_τ, y'_μ, and Y_{45}. We need to examine if they will be further constrained by other rare decays. Since the new physics effects occur in the lepton sector, the strict constraints may come from the lepton-flavor violating processes, such as $\tau \to 3\mu$, $\tau \to (e,\mu)\gamma$, and $\mu \to e\gamma$. From Eq. (44), it is known that $\tau \to 3\mu$ can be induced through off-shell h decay into the muon pair. The BR for this three-body decay can be expressed as:

$$BR(\tau \to 3\mu) = \frac{\tau_\tau m_\tau^5}{3 \cdot 2^9 \pi^3 m_h^4} |y_{\mu\mu} a_R|^2 \approx 1.2 \times 10^{-7} |a_R|^2 , \tag{49}$$

where $y_{\mu\mu} = m_\mu / v_H$ is the Higgs coupling to the muon in the SM, and the small a_L has been ignored. Taking $a_R \approx 10^{-3}$, the h-mediated $BR(\tau \to 3\mu)$ is much less than the current upper bound of 2.1×10^{-8} [5]. To induce the rare $\mu \to e\gamma$ process, the new Yukawa couplings have to couple to the electron. From Eqs. (2) and (5), the relevant couplings are Y_{ee}, y_e, and y'_e, however, $Y_{ee} \approx y_e \approx 0$ and $y'_e \ll 1$ have been used to fit the neutrino masses. Thus, the rare $\mu \to e\gamma$ process is suppressed in our model.

Similarly, $\tau \to (e,\ \mu)\gamma$ are suppressed by most Yukawa couplings with the exception of y_τ and y'_μ, where the associated Feynman diagram is shown in Fig. 5. It can be seen that in addition to y_τ and y'_μ, the quartic scalar coupling λ_{10} involves in the $\tau \to \mu\gamma$ process. As a result, the interaction of the loop induced $\tau \to \mu\gamma$ can be written as:

$$\mathcal{L}_{\tau\mu\gamma} = -\frac{e m_\tau}{16\pi^2} C_R \bar{\mu} \sigma_{\mu\nu} P_R \tau F^{\mu\nu} , \ C_R = \frac{\lambda_{10} v_H a_R}{2 m_\tau m_L^2} I(z_h, z_S) , \tag{50}$$

$$I(z_h, z_S) = \int_0^1 dx_1 \int_0^{x_1} dx_2 \frac{x_2^2}{(z_h - (z_h - z_S)x_1 + (1 - z_S)x_2)^2} ,$$

with $z_h = m_h^2/m_L^2$ and $z_S = m_S^2/m_L^2$. The BR for $\tau \to \mu\gamma$ can be expressed as:

$$\frac{BR(\tau \to \mu\gamma)}{BR(\tau \to \mu \bar{\nu}_\mu \nu_\tau)} = \frac{3\alpha_e}{4\pi G_F} |C_R|^2 \approx 1.51 \times 10^{-13} \left(\frac{|a_R| \lambda_{10}}{10^{-3}} \right)^2 , \tag{51}$$

where we have used $a_R \approx 10^{-3}$, $m_h \approx 125$ GeV, $m_S \approx 10$ GeV, $m_L \approx 1000$ GeV, and $I(z_h, z_S) \approx 0.46$. Clearly, the BR for $\tau \to \mu\gamma$ in our model is still below the current upper bound of 4.4×10^{-8} [5]. Note that we have ignored the a_L effect due to the use of $a_L \ll a_R$.

5.3. Phenomenological implications on the muon $g-2$, rare τ, and $H^{--} \to \mu\tau$ decays

After determining the magnitudes of the Higgs-triplet Yukawa couplings, which are used to explain the neutrino data, we state some implications of this model in flavor and collider physics, which have been studied in the literature and are still interesting in this model. In addition to the large $BR(h \to \mu\tau)$, if the new Z' gauge boson is in the MeV to GeV range, the muon $g-2$ anomaly can be resolved by the intermediate Z'-gauge boson [26,27,33], depending on the magnitude of $g_{Z'}$ gauge coupling. The contribution from the Z'-penguin diagram to the muon $g-2$ can be expressed as [26,33]

$$\Delta a_\mu^{Z'} = \frac{g_{Z'}^2}{8\pi^2} \int_0^1 dx \frac{2m_\mu^2 x^2(1-x)}{x^2 m_\mu^2 + (1-x)m_{Z'}^2}. \tag{52}$$

It is found that to explain the muon $g-2$ anomaly, $\Delta a_\mu = a_\mu^{\rm exp} - a_\mu^{\rm SM} = (28.7 \pm 8.0) \times 10^{-10}$ [5], the allowed ranges of $g_{Z'}$ and $m_{Z'}$ are :

$$2 \times 10^{-4} \leq g_{Z'} \leq 2 \times 10^{-3}, \tag{53}$$

$$5 \leq m_{Z'} \leq 210 \text{ MeV}, \tag{54}$$

where other regions have been experimentally excluded, such as the neutrino trident production [70], BABAR collaboration [71], and Borexino experiment [72].

With the value of $a_R \sim 10^{-3}$, the sizable Yukawa couplings y'_μ and y_τ can induce the lepton-flavor violating interaction τ-μ-S through the mixing between vector-like lepton and $\tau(\mu)$-lepton. From the S-Z'-Z' interaction, the $\tau \to \mu Z' Z'$ decay can be generated by the mediation of light scalar S, and its partial decay rate as a function of Z'-pair invariant can be derived as [34]:

$$\frac{dBR(\tau \to \mu Z' Z')}{dq^2} \approx \frac{m_\tau}{64\pi^2 m_h} \frac{\Gamma_h}{\Gamma_\tau} BR(h \to \mu\tau) \times \frac{(q^2 - 2m_{Z'}^2)^2 + 8m_{Z'}^4}{v_S^4 m_S^2} \left(1 - \frac{q^2}{m_\tau^2}\right)^2 \sqrt{1 - \frac{4m_{Z'}^2}{q^2}}. \tag{55}$$

It can be seen that $\tau \to \mu Z' Z'$ and $h \to \mu\tau$ can be correlated in the model when $m_{Z'}$ is below GeV. We show the $BR(\tau \to \mu Z' Z')$ (in units of 10^{-9}) as a function of $BR(h \to \mu\tau)$ (in units of 10^{-3}) and v_S in Fig. 6, where $m_S = 10$ GeV and $m_{Z'} = 0.2$ GeV are fixed. With 50 ab^{-1} of data accumulated at the Belle II, the sample of τ pairs can be increased up to around 5×10^{10}, where the sensitivity necessary to observe the LFV τ decays can reach $10^{-10} - 10^{-9}$ [69]. Therefore, the $BR(\tau \to \mu Z' Z')$ of 10^{-9} allowed in the model could be tested at the Belle II.

Moreover, we find that a sizable Y_{45} Yukawa coupling can change the decay property of doubly charged Higgs $H^{\pm\pm}$ in the Higgs triplet. In this model, $H^{\pm\pm}$ can decay to the $\mu^\pm\tau^\pm$ final states via the dimension-4 and the induced dimension-6 operators, which are expressed as:

$$Y_{\mu\tau} L_\mu^T C i\tau_2 \Delta L_\tau + \frac{Y_{45} y_\tau y_\mu}{m_L^2} \tau_R^T H^T i\tau_2 \Delta H \mu_R, \tag{56}$$

where the corresponding $H^{\pm\pm}$ Yukawa coupling to $\mu^\pm\tau^\pm$ can be written as:

$$Y_{H^{\pm\pm}} = Y_{\mu\tau}^* + Y_{45} y_\tau y_\mu \frac{v_H^2}{2m_L^2}. \tag{57}$$

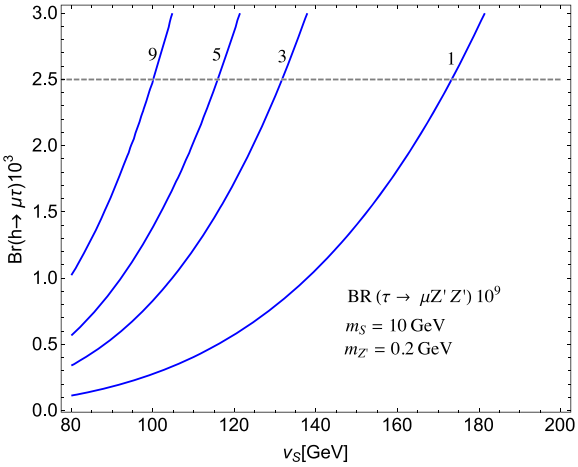

Fig. 6. Correlation between $BR(h \to \mu\tau)$ (in units of 10^{-3}) and $BR(\tau \to \mu Z' Z')$ (in units of 10^{-9}, where the horizontal dashed line is the upper bound of $h \to \mu\tau$, and we have fixed $m_S = 10$ GeV and $m_{Z'} = 0.2$ GeV.

From Eq. (48), Y_{45} can in principle be $O(0.1)$ when other neutrino mass related parameters are tuned to be small, e.g. $Y_{\mu\tau} v_\Delta/\sqrt{2} \sim 10^{-10}$. Thus, with $m_L \approx 1000$ GeV, $v_H \approx 246$ GeV, $m_{H^{\pm\pm}} \approx 800$ GeV, and $y_\tau \sim y_\mu \sim 0.1$, the decay rate ratio of $H^{\pm\pm} \to \mu^\pm\tau^\pm$ to $H^{\pm\pm} \to W^\pm W^\pm$ can be estimated as [73]:

$$\frac{\Gamma(H^{\pm\pm} \to \mu^\pm\tau^\pm)}{\Gamma(H^{\pm\pm} \to W^\pm W^\pm)} \approx \frac{|Y_{H^{\pm\pm}}|^2 v_H^2}{2v_\Delta^2} \frac{v_H^2}{m_{H^{\pm\pm}}^2} \approx \frac{2.6 \times 10^{-4} |Y_{45}|^2}{v_\Delta^2}, \tag{58}$$

where the small $Y_{\mu\tau}$ is neglected. With $|Y_{45}| \sim 0.05$ and $v_\Delta \sim 0.01$ GeV, the ratio can be at the 10% level; that is, the BR for $H^{\pm\pm} \to \mu^\pm\tau^\pm$ is not suppressed and can be a good channel to observe the doubly charged-Higgs. In addition, the $\tau \to \ell_i \ell_j \bar{\ell}_k$ decays can be induced by the $H^{\pm\pm}$ couplings shown in Eq. (56). Since we focus on the $\mathcal{A}_1$ pattern, the potential mode is $\tau \to \mu\mu\bar{\mu}$ and its BR can be estimated as [74]:

$$\frac{BR(\tau \to \mu\mu\bar{\mu})}{BR(\tau \to \mu\bar{\nu}\nu)} = \frac{1}{4G_F^2 m_{H^{\pm\pm}}^4} |Y_{H^{\pm\pm}}|^2 \left(\frac{\sqrt{2} m_{\mu\mu}}{v_\Delta}\right)^2. \tag{59}$$

This BR is tiny since it is suppressed by $(m_{\mu\mu}/v_\Delta)^2 \sim 4 \times 10^{-17}$ when $v_\Delta \sim 0.01$ GeV is used; therefore, this process cannot give a strict constraint on $Y_{H^{\pm\pm}}$.

6. Summary

We studied the origin of the neutrino mass in the gauged $L_\mu - L_\tau$ model. We learned that although including one Higgs triplet can violate the lepton number, the effect is not sufficient to explain the neutrino data due to the $U(1)_{L_\mu - L_\tau}$ gauge invariance. It was found that a proper symmetric Majorana mass matrix can be obtained when a pair of vector-like leptons and two singlet scalars, which carry the $L_\mu - L_\tau$ charges, are introduced. In this model, a specific Frampton–Glashow–Marfatia matrix pattern can be achieved when some Yukawa couplings are set to vanish. Using the pattern $\mathbf{A}_1$, we showed that when the neutrino data within 1σ errors and cosmological neutrino bound are satisfied, the involving Higgs-triplet Yukawa couplings have

a hierarchy, i.e., $Y_{\mu\tau} \ll Y_{\mu 4} \ll Y_{\tau 5} \ll Y_{45}$, and Y_{45} can be $O(0.1)$. As a result, the effective Majorana neutrino mass is below the upper limit of neutrinoless double-beta decay experiment. Moreover, when the neutrino data are satisfied, it was found that the model can exhibit interesting phenomena in flavor and collider physics, such as muon $g-2$, $h \to \mu\tau$, $\tau \to \mu Z' Z'$, and $H^{\pm\pm} \to (W^{\pm}W^{\pm}, \mu^{\pm}\tau^{\pm})$ decays, although they are not new findings in this paper.

Acknowledgements

This work was partially supported by the Ministry of Science and Technology of Taiwan, under grant MOST-103-2112-M-006-004-MY3 (CHC).

References

[1] F. Englert, R. Brout, Phys. Rev. Lett. 13 (1964) 321.
[2] P.W. Higgs, Phys. Rev. Lett. 13 (1964) 508.
[3] G. Aad, et al., ATLAS Collaboration, Phys. Lett. B 716 (2012) 1, arXiv:1207.7214 [hep-ex].
[4] S. Chatrchyan, et al., CMS Collaboration, Phys. Lett. B 716 (2012) 30, arXiv:1207.7235 [hep-ex].
[5] C. Patrignani, et al., Particle Data Group, Chin. Phys. C 40 (2016) 100001.
[6] B. Pontecorvo, Sov. Phys. JETP 6 (1957) 429, Zh. Eksp. Teor. Fiz. 33 (1957) 549.
[7] Z. Maki, M. Nakagawa, S. Sakata, Prog. Theor. Phys. 28 (1962) 870.
[8] N. Cabibbo, Phys. Rev. Lett. 10 (1963) 531.
[9] M. Kobayashi, T. Maskawa, Prog. Theor. Phys. 49 (1973) 652.
[10] P. Minkowski, Phys. Lett. B 67 (1977) 421;
T. Yanagida, Proceedings of the Workshop on Unified Theories and Baryon Number in the Universe, A. Sawada, A. Sugamoto (Eds.), KEK Report No. 79-18, 1979;
S. Glashow, in: M. Lévy, et al. (Eds.), Quarks and Leptons, Cargese, 1979, Plenum, New York, 1980;
M. Gell-Mann, P. Ramond, R. Slansky, in: Proceedings of the Supergravity Stony Brook Workshop, New York, in: P. Van Nieuwenhuizen, D. Freedman, North-Holland, Amsterdam, 1979;
R.N. Mohapatra, G. Senjanović, Phys. Rev. Lett. 44 (1980) 912.
[11] P. Binetruy, S. Lavignac, S.T. Petcov, P. Ramond, Nucl. Phys. B 496 (1997) 3, arXiv:hep-ph/9610481.
[12] R.N. Mohapatra, A. Perez-Lorenzana, C.A. de Sousa Pires, Phys. Lett. B 474 (2000) 355, arXiv:hep-ph/9911395.
[13] W. Grimus, L. Lavoura, Phys. Rev. D 62 (2000) 093012, arXiv:hep-ph/0007011.
[14] N.F. Bell, R.R. Volkas, Phys. Rev. D 63 (2001) 013006, arXiv:hep-ph/0008177.
[15] K.S. Babu, R.N. Mohapatra, Phys. Lett. B 532 (2002) 77, arXiv:hep-ph/0201176.
[16] H.S. Goh, R.N. Mohapatra, S.P. Ng, Phys. Lett. B 542 (2002) 116, arXiv:hep-ph/0205131.
[17] S.T. Petcov, W. Rodejohann, Phys. Rev. D 71 (2005) 073002, arXiv:hep-ph/0409135.
[18] W. Grimus, L. Lavoura, J. Phys. G 31 (2005) 683, arXiv:hep-ph/0410279.
[19] S. Choubey, W. Rodejohann, Eur. Phys. J. C 40 (2005) 259, arXiv:hep-ph/0411190.
[20] B. Adhikary, Phys. Rev. D 74 (2006) 033002, arXiv:hep-ph/0604009.
[21] K. Asai, K. Hamaguchi, N. Nagata, arXiv:1705.00419 [hep-ph].
[22] X.G. He, G.C. Joshi, H. Lew, R.R. Volkas, Phys. Rev. D 43 (1991) 22.
[23] R. Foot, X.G. He, H. Lew, R.R. Volkas, Phys. Rev. D 50 (1994) 4571, arXiv:hep-ph/9401250.
[24] S.N. Gninenko, N.V. Krasnikov, Phys. Lett. B 513 (2001) 119, arXiv:hep-ph/0102222.
[25] S.N. Gninenko, N.V. Krasnikov, V.A. Matveev, Phys. Rev. D 91 (2015) 095015, arXiv:1412.1400 [hep-ph].
[26] W. Altmannshofer, C.Y. Chen, P.S. Bhupal Dev, A. Soni, Phys. Lett. B 762 (2016) 389, arXiv:1607.06832 [hep-ph].
[27] W. Altmannshofer, S. Gori, M. Pospelov, I. Yavin, Phys. Rev. D 89 (2014) 095033, arXiv:1403.1269 [hep-ph].
[28] A. Crivellin, G. D'Ambrosio, J. Heeck, Phys. Rev. Lett. 114 (2015) 151801, arXiv:1501.00993 [hep-ph].
[29] W. Altmannshofer, S. Gori, S. Profumo, F.S. Queiroz, J. High Energy Phys. 1612 (2016) 106, arXiv:1609.04026 [hep-ph].
[30] P. Ko, T. Nomura, H. Okada, Phys. Rev. D 95 (11) (2017) 111701, arXiv:1702.02699 [hep-ph].
[31] C.H. Chen, T. Nomura, Phys. Lett. B 777 (2018) 420, arXiv:1707.03249 [hep-ph].
[32] Y. Kaneta, T. Shimomura, PTEP 2017, no. 5, 053B04, arXiv:1701.00156 [hep-ph], 2017.
[33] T. Araki, S. Hoshino, T. Ota, J. Sato, T. Shimomura, Phys. Rev. D 95 (5) (2017) 055006, arXiv:1702.01497 [hep-ph].
[34] C.H. Chen, T. Nomura, Phys. Rev. D 96 (9) (2017) 095023, arXiv:1704.04407 [hep-ph].

[35] J. Heeck, W. Rodejohann, Phys. Rev. D 84 (2011) 075007, arXiv:1107.5238 [hep-ph].
[36] J. Heeck, M. Holthausen, W. Rodejohann, Y. Shimizu, Nucl. Phys. B 896 (2015) 281, arXiv:1412.3671 [hep-ph].
[37] S. Baek, H. Okada, K. Yagyu, J. High Energy Phys. 1504 (2015) 049, arXiv:1501.01530 [hep-ph].
[38] S. Baek, Phys. Lett. B 756 (2016) 1, arXiv:1510.02168 [hep-ph].
[39] J. Heeck, Phys. Lett. B 758 (2016) 101, arXiv:1602.03810 [hep-ph].
[40] W. Altmannshofer, M. Carena, A. Crivellin, Phys. Rev. D 94 (9) (2016) 095026, arXiv:1604.08221 [hep-ph].
[41] S. Patra, S. Rao, N. Sahoo, N. Sahu, Nucl. Phys. B 917 (2017) 317, arXiv:1607.04046 [hep-ph].
[42] A. Biswas, S. Choubey, S. Khan, J. High Energy Phys. 1609 (2016) 147, arXiv:1608.04194 [hep-ph].
[43] S. Lee, T. Nomura, H. Okada, arXiv:1702.03733 [hep-ph].
[44] M. Magg, C. Wetterich, Phys. Lett. B 94 (1980) 61;
G. Lazarides, Q. Shafi, C. Wetterich, Nucl. Phys. B 181 (1981) 287;
R.N. Mohapatra, G. Senjanovic, Phys. Rev. D 23 (1981) 165;
E. Ma, U. Sarkar, Phys. Rev. Lett. 80 (1998) 5716, arXiv:hep-ph/9802445.
[45] W. Konetschny, W. Kummer, Phys. Lett. B 70 (1977) 433;
J. Schechter, J.W.F. Valle, Phys. Rev. D 22 (1980) 2227;
T.P. Cheng, L.-F. Li, Phys. Rev. D 22 (1980) 2860;
S.M. Bilenky, J. Hosek, S.T. Petcov, Phys. Lett. B 94 (1980) 495.
[46] E.J. Chun, H.M. Lee, P. Sharma, J. High Energy Phys. 1211 (2012) 106, arXiv:1209.1303 [hep-ph].
[47] M. Baak, et al., Gfitter Group, Eur. Phys. J. C 74 (2014) 3046, arXiv:1407.3792 [hep-ph].
[48] D. Das, A. Santamaria, Phys. Rev. D 94 (1) (2016) 015015, arXiv:1604.08099 [hep-ph].
[49] The ATLAS collaboration [ATLAS Collaboration], ATLAS-CONF-2018-028.
[50] A.M. Sirunyan, et al., CMS Collaboration, arXiv:1804.02716 [hep-ex].
[51] S. Dittmaier, et al., LHC Higgs Cross Section Working Group, arXiv:1101.0593 [hep-ph].
[52] G. Aad, et al., ATLAS Collaboration, J. High Energy Phys. 1511 (2015) 206, arXiv:1509.00672 [hep-ex].
[53] V. Khachatryan, et al., CMS Collaboration, J. High Energy Phys. 1702 (2017) 135, arXiv:1610.09218 [hep-ex].
[54] C.H. Chen, T. Nomura, J. High Energy Phys. 1409 (2014) 120, arXiv:1404.2996 [hep-ph].
[55] P.H. Frampton, S.L. Glashow, D. Marfatia, Phys. Lett. B 536 (2002) 79, arXiv:hep-ph/0201008.
[56] I. Dorsner, S. Fajfer, A. Greljo, J.F. Kamenik, N. Kosnik, I. Nisandzic, J. High Energy Phys. 1506 (2015) 108, arXiv:1502.07784 [hep-ph].
[57] J. Herrero-Garcia, N. Rius, A. Santamaria, J. High Energy Phys. 1611 (2016) 084, arXiv:1605.06091 [hep-ph].
[58] H. Fritzsch, Z.z. Xing, S. Zhou, J. High Energy Phys. 1109 (2011) 083, arXiv:1108.4534 [hep-ph].
[59] D. Meloni, G. Blankenburg, Nucl. Phys. B 867 (2013) 749, arXiv:1204.2706 [hep-ph].
[60] P.O. Ludl, W. Grimus, J. High Energy Phys. 1407 (2014) 090, arXiv:1406.3546 [hep-ph], Erratum: J. High Energy Phys. 1410 (2014) 126.
[61] L.M. Cebola, D. Emmanuel-Costa, R.G. Felipe, Phys. Rev. D 92 (2) (2015) 025005, arXiv:1504.06594 [hep-ph].
[62] S. Vagnozzi, E. Giusarma, O. Mena, K. Freese, M. Gerbino, S. Ho, M. Lattanzi, Phys. Rev. D 96 (12) (2017) 123503, arXiv:1701.08172 [astro-ph.CO].
[63] F. Couchot, S. Henrot-Versille, O. Perdereau, S. Plaszczynski, B. Rouille d'Orfeuil, M. Spinelli, M. Tristram, Astron. Astrophys. 606 (2017) A104, arXiv:1703.10829 [astro-ph.CO].
[64] F. Capozzi, E. Di Valentino, E. Lisi, A. Marrone, A. Melchiorri, A. Palazzo, Phys. Rev. D 95 (9) (2017) 096014, arXiv:1703.04471 [hep-ph].
[65] A. Gando, et al., KamLAND-Zen Collaboration, Phys. Rev. Lett. 117 (8) (2016) 082503, arXiv:1605.02889 [hep-ex], Addendum: Phys. Rev. Lett. 117 (10) (2016) 109903.
[66] G. Aad, et al., ATLAS Collaboration, Eur. Phys. J. C 77 (2) (2017) 70, arXiv:1604.07730 [hep-ex].
[67] V. Khachatryan, et al., CMS Collaboration, Phys. Lett. B 749 (2015) 337, arXiv:1502.07400 [hep-ex].
[68] CMS Collaboration [CMS Collaboration], CMS-PAS-HIG-17-001.
[69] T. Aushev, et al., arXiv:1002.5012 [hep-ex].
[70] W. Altmannshofer, S. Gori, M. Pospelov, I. Yavin, Phys. Rev. Lett. 113 (2014) 091801, arXiv:1406.2332 [hep-ph].
[71] J.P. Lees, et al., BaBar Collaboration, Phys. Rev. D 94 (1) (2016) 011102, arXiv:1606.03501 [hep-ex].
[72] G. Bellini, et al., Phys. Rev. Lett. 107 (2011) 141302, arXiv:1104.1816 [hep-ex].
[73] T. Han, B. Mukhopadhyaya, Z. Si, K. Wang, Phys. Rev. D 76 (2007) 075013, arXiv:0706.0441 [hep-ph].
[74] A.G. Akeroyd, M. Aoki, H. Sugiyama, Phys. Rev. D 79 (2009) 113010, arXiv:0904.3640 [hep-ph].